11th International Symposium on Turbulence and Shear Flow Phenomena (TSFP11)
Southampton, UK, July 30 to August 2, 2019

REYNOLDS-NUMBER DEPENDENCE OF THE TOWNSEND-PERRY 'CONSTANT' IN WALL TURBULENCE

Sourabh S. Diwan
Department of Aerospace Engineering
Indian Institute of Science
Bangalore 560012
sdiwan@iisc.ac.in

Jonathan F. Morrison
Department of Aeronautics
Imperial College London
South Kensington, London SW7 2AZ
j.morrison@imperial.ac.uk

ABSTRACT

We address the question of Reynolds-number dependence of the "Townsend-Perry constant", which is the slope of the logarithmic variation of the streamwise variance in wall turbulence. We make use of the turbulent pipe flow and boundary layer (TBL) data available in the literature. We find that using a wall-normal length scale, proportional to the square root of the friction Reynolds number (akin to the distance of the "mesolayer" from the wall) and an associated velocity scale, it is possible to obtain a Reynolds-number similarity for the streamwise variance in a region intermediate to the inner and outer layers. In this region, the intermediate-scaled variance follows a logarithmic variation for which the coefficients are independent of Reynolds number, and the extent of the log region increases with increase in Reynolds number. The intermediate-scaled log-law constants for the pipe and TBL are fairly close to each other, suggesting a plausible "universal" behaviour for the variance, in terms of the intermediate variables. The consequence of Re-number invariance of the intermediate-scaled log law is that the classical Townsend-Perry 'constant' shows a systematic variation with Reynolds number. For the pipe flow the Townsend-Perry 'constant' is seen to increase until the highest Reynolds number, whereas for the TBL it reaches a relatively constant value for sufficiently large Reynolds numbers. These are interesting findings, which can have important implications towards understanding the scaling and structure of the high-Reynolds-number wall turbulence; in particular, their implications for the attached-eddy modelling are briefly discussed.

INTRODUCTION

Townsend (1976) proposed the attached eddy hypothesis for the inertial sublayer in wall-bounded turbulent flows (e.g., boundary layer, channel and pipe flows), valid for asymptotically large Reynolds numbers. He considered a random distribution of eddies to describe the statistics of wall turbulence, with a given eddy size proportional to the distance from the wall and its population density inversely proportional to the distance from the wall. Using the friction velocity, $u_\tau = \sqrt{\tau_w/\rho}$, as the velocity scale for the range of "attached" eddies, Townsend (1976) arrived at a logarithmic profile for the streamwise (and spanwise) velocity variance in the inertial sublayer, given as

$$\frac{\overline{u^2}}{u_\tau^2} = B_1 - A_1 \ln\left(\frac{y}{\delta}\right). \tag{1}$$

Here u is fluctuating streamwise velocity, τ_w is wall shear stress, ρ is density, y is wall-normal location, and δ is a measure of the thickness of the wall-bounded flow. For the pipe flow, $\delta = R$, the pipe radius and for the turbulent boundary layer (TBL), $\delta = \delta_{99}$, the 99% boundary-layer thickness; the overbar indicates time averaging. A_1 in equation (1) is the "Townsend-Perry constant", which, within the attached-eddy framework, is believed to be a universal constant (Marusic *et al.*, 2013).

The first successful attempt at developing a kinematic model for wall turbulence, based on the attached-eddy hypothesis, was made by Perry & Chong (1982), who used a hierarchy of hairpin-shaped eddies to calculate the statistics. The attached-eddy model of Perry & Chong (1982) reproduced the logarithmic variation of the mean velocity and streamwise variance as dual conditions. Many further developments of this model have been carried out subsequently, e.g. Perry *et al.* (1986), Perry & Marusic (1995) among others; the current state of understanding has been reviewed by Marusic & Monty (2019).

Testing the universality and Reynolds-number invariance of the Townsend-Perry constant (A_1) is an area of active research. For the experiments of Perry *et al.* (1986) in the pipe flow, A_1 was found to be 0.9 for the friction Reynolds numbers. $Re_\tau = R^+ = u_\tau R/\nu \leq 3{,}900$. Here superscript $^+$ indicates the wall scaling. Perry & Li (1990) found $A_1 = 1.03$ for the TBL for $Re_\tau = \delta_{99}^+ = 1{,}193 - 4{,}433$. This value for A_1 has been quoted in subsequent studies on TBL. For example, Nickels *et al.* (2007) used $A_1 = 1.03$, assuming it to be Reynolds-number indepen-

dent, to describe the variation of $\overline{u^2}$ with Re_τ (at $y^+ = 300$), for $Re_\tau = 2,000 - 20,000$. $A_1 = 1.03$ as a representative value for the TBL also appears in Smits *et al.* (2011). More recently, Marusic *et al.* (2013) used the data from high Reynolds number wall turbulence and found A_1 to be 1.23 ± 0.05 for the pipe and 1.26 ± 0.06 for TBL. Meneveau & Marusic (2013) obtained $A_1 = 1.25$ for $Re_\tau = 2,498 - 6,494$ and 1.19 for $Re_\tau \approx 16000$ for the TBL. Vallikivi *et al.* (2015) used $A_1 = 1.24$ for both pipe and TBL at $Re_\tau > 20,000$, but did not determine the uncertainty limits on this value.

In summary, A_1 appears to depend on Reynolds number, at least for low Re_τ, and therefore, by implication, on the nature of the outer boundary condition. However, it is not entirely clear if A_1 is a systematic function of Re_τ and this is the question we would like to address here. Towards this objective, we take a close look at the scaling behaviour of the streamwise variance in an intermediate region between the inner and outer layers for the high-Reynolds-number data on pipe flow and TBL available in the literature. We find that the length scale appropriate for the intermediate region, y_m^+, is proportional to $\sqrt{Re_\tau}$, which is the typical "mesolayer" scaling (Sreenivasan & Sahay, 1997; Klewicki, 2013). The velocity scale (u_m) is chosen to be the rms turbulence velocity at $y = y_m$. For the present purposes, the intermediate region is defined as a region around $y/y_m = 1$ that is described by the scaling variables y_m and u_m. We prefer to call this region as "intermediate" region/layer to distinguish it from the several different connotations associated with the term "mesolayer" used in the literature.

With the above length and velocity scales, the streamwise variance in the intermediate region of the pipe flow and TBL shows a Reynolds-number similarity, to an excellent degree, for Re_τ varying over two decades ($O(10^3) - O(10^5)$). The implication of this finding is that A_1 in equation (1) exhibits a systematic Reynolds-number dependence; for the pipe this continues until the highest Reynolds number, whereas for the TBL, A_1 appears to reach a relatively constant value for high Reynolds numbers.

SCALING FOR THE INTERMEDIATE REGION

In the following analysis we use the turbulent pipe-flow data obtained in Princeton Superpipe using NSTAP (Hultmark *et al.*, 2012, 2013). For the TBL, we use two data sets - one obtained in the HRTF experiments at Princeton university (Vallikivi *et al.*, 2015, VHS) and the other obtained in the HRNBLWT experiments at Melbourne University (Mathis *et al.*, 2009, MHM). The data measured at Princeton have been made available for use at *https://smits.princeton.edu/data-sets/*.

To explore the scaling behaviour of the streamwise variance in the intermediate region of the pipe flow, we choose the length scale to be $y_m^+ = 3.5\sqrt{Re_\tau}$ and the velocity scale $u_m = \sqrt{\overline{u^2}}(y = y_m)$. The variance profiles scaled on these variables, for the smooth-pipe data of Hultmark *et al.* (2012), are shown in figure 1. There is an excellent collapse of the profiles in a region around $y/y_m = 1$ across the entire range of Reynolds numbers spanning two decades ($1,985 - 98,190$). For the highest Reynolds numbers, the scaling region extends from $0.15 \le y/y_m \le 15$ and the profiles peel off from this trend on both the sides of $y/y_m = 1$ as Re_τ decreases.

In figure 2, we plot the variance measured in a rough-wall pipe flow, reported in Hultmark *et al.* (2013), using the same choice of y_m and u_m as for the smooth pipe. Figure 2 also shows the smooth-wall variance profiles for comparison. In the region for $y > y_m$, the rough-wall profiles exhibit Reynolds-number invariance over a decade of $Re_\tau(19,316 - 100,530)$. Moreover, in this region, the rough-wall pipe data collapses very well on the smooth pipe data, indicating that the intermediate-scaled variance is independent of the surface condition. Note that the rough-wall profiles do not show good collapse for $y < y_m$, probably due to the wall being transitionally rough (Hultmark *et al.*, 2013).

Figure 3 shows the TBL data on streamwise variance scaled on $y_m^+ = 3.5\sqrt{Re_\tau}$ and $u_m = \sqrt{\overline{u^2}}(y = y_m)$ – with the same coefficient used in the definition of y_m for the pipe flow. Again there is a good collapse of the data across the entire range of Reynolds numbers in the neighbourhood of y_m, especially for $y/y_m > 1$. For $y/y_m < 1$, the data of MHM show a good scaling but the data of VHS do not show the same degree of collapse; the reason for this behaviour is not entirely clear. Note that the Reynolds-number range originally specified in Mathis *et al.* (2009) is $2,800 - 19,000$. However, this is based on a different definition of boundary-layer thickness, say δ_1, which was calculated from a modified Coles law of the wake fit (Mathis *et al.*, 2009). An assessment of the data of MHM shows that $\delta_1 \approx 1.2\delta_{99}$ and this relation has been used to obtain Re_τ based on δ_{99} in this work (figure 3).

Selection of the constant used in the definition of y_m above is motivated by the coefficients for $\sqrt{Re_\tau}$ previously used in the definition of the mesolayer location ($2\sqrt{Re_\tau}$ as in Sreenivasan & Sahay, 1997) or in determining the lower bound of the inertial sublayer ($3\sqrt{Re_\tau}$ as in Marusic *et al.*, 2013). A slightly higher value of 3.5 was chosen here as it provides a better Re_τ scaling of the variance profiles for both pipe and boundary layer data. Note that the qualitative (and, to certain extent quantitative) nature of the results is unaffected by the precise choice of this constant.

LOG LAW FOR STREAMWISE VARIANCE

The Reynolds-number similarity for the variance around $y = y_m$ in figures 1, 2 (pipe flow) and figure 3 (TBL) implies that, for $y > y_m$, there should exist a Reynolds-number-independent log law for the variance scaled on the intermediate variables, given as

$$\frac{\overline{u^2}}{u_m^2} = B_1^m - A_1^m \ln\left(\frac{y}{y_m}\right). \tag{2}$$

For the data in figure 1 the extent of this log law is seen to be in the range $1.2 \le y/y_m \le 13$, or $4.2\sqrt{Re_\tau} \le y^+ \le 0.145Re_\tau$ for $Re_\tau = 98,190$, which is broadly consistent with Marusic *et al.* (2013). As Re_τ decreases, the extent of the variance profile in the log-law region continues to decrease. To determine the constants A_1^m and B_1^m in equation (2) for the pipe flow, we fit a least-squares straight line through the points in figure 1 (shown as a solid line) in the region $1.2 \le y/y_m \le 13$ for the two highest Reynolds numbers. This gives $A_1^m = 0.178$ and $B_1^m = 1.005$ for the pipe flow, both of which are Reynolds-number invariant.

For the TBL data in figure 3, a straight-line is fitted in the region $1.5 \le y/y_m \le 10$ for the highest Reynolds numbers from each of the data sets, i.e. $Re_\tau = 15,685$ for MHM

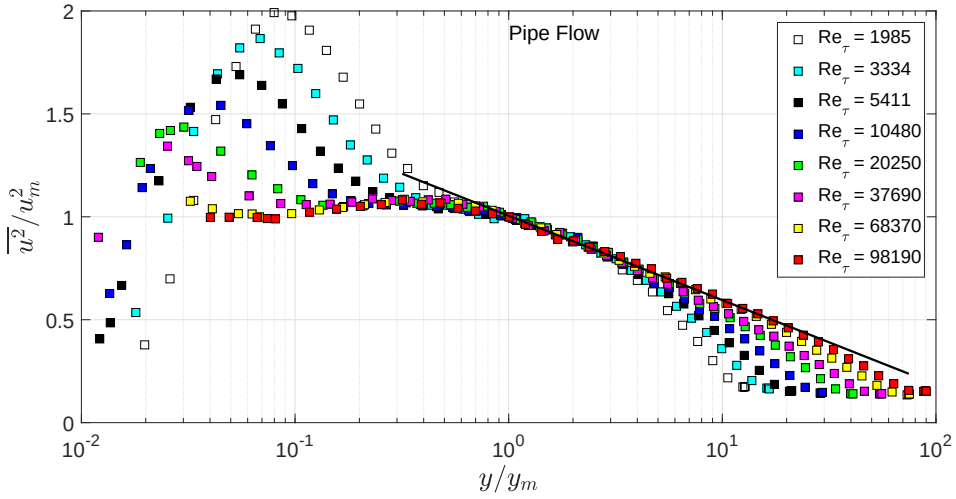

Figure 1. Streamwise variance profiles in smooth pipe scaled y_m and u_m; data from Hultmark *et al.* (2012). Here $Re_\tau = R^+$. The solid line is the log-law fit (equation 2), with $A_1^m = 0.178$ and $B_1^m = 1.005$.

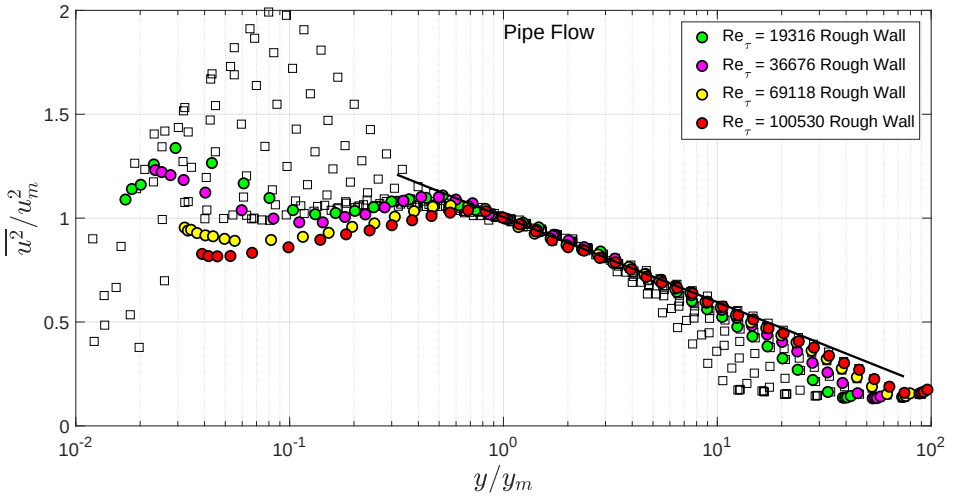

Figure 2. Streamwise variance profiles in rough pipe scaled on y_m and u_m; data from Hultmark *et al.* (2013). The open squares correspond to the smooth-pipe data. The solid line is the log-law fit (equation 2), with $A_1^m = 0.178$ and $B_1^m = 1.005$.

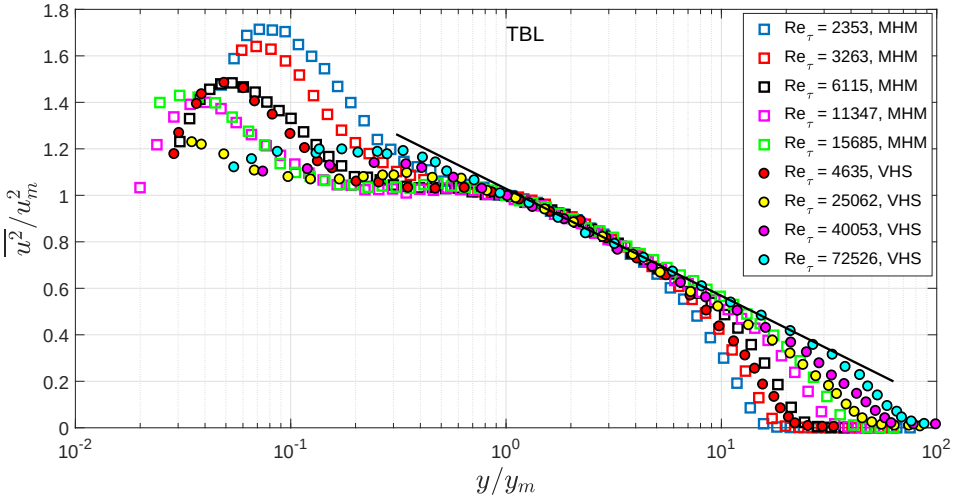

Figure 3. Streamwise variance profiles in the TBL scaled on y_m and u_m; data from Mathis *et al.* (2009)- MHM and Vallikivi *et al.* (2015)- VHS. Here $Re_\tau = \delta_{99}^+$. The solid line is the log-law fit (equation 2), with $A_1^m = 0.200$ and $B_1^m = 1.028$.

Table 1. Summary of the log-law constants for pipe and TBL, along with averaged values which could represent the plausible "universal" constants.

Case	A_1^m	B_1^m
Turbulent pipe flow	0.178	1.005
Turbulent boundary layer	0.200	1.028
Plausible 'universal' values	0.189	1.017

and $Re_\tau = 72,526$ for VHS. This gives $A_1^m = 0.200$ and $B_1^m = 1.028$ for the TBL. We could have as well chosen the two highest Reynolds numbers for VHS, i.e. $Re_\tau = 40,053$ and $72,526$, for fitting a straight line, which gives slightly different numbers for the log-law constants ($A_1^m = 0.204$ and $B_1^m = 1.020$). However since we have used two different data sets for the TBL, the choice of $A_1^m = 0.200$ and $B_1^m = 1.028$ gives a more representative fit for the two sets (solid line in figure 3), and we use these numbers in the following.

Note that, provided the Reynolds-number similarity in the intermediate region is correct, the value of A_1^m is independent of the choice of the numerical constant in the definition of y_m; the value of B_1^m, however, depends on this choice (equation 2). Furthermore, the precise values of A_1^m and B_1^m would depend upon the range of y/y_m chosen to fit the log law. However, the precise values of A_1^m and B_1^m are not relevant to the main conclusion of this paper and therefore we do not attempt to determine uncertainty bounds on these constants.

The numerical values of A_1^m and B_1^m obtained above for the pipe flow and TBL are quite close to each other and it is therefore interesting to ask if the intermediate scaling exhibits a 'universal' behaviour. In figure 4, we compare the variance profiles for the pipe flow and TBL, with intermediate scaling. A fairly good degree of collapse is observed near y_m for $y/y_m > 1$; there is much more scatter for $y/y_m < 1$. The solid line corresponds to the log-law fit using constants: $A_1^m = 0.189$ and $B_1^m = 1.017$, obtained by averaging over the corresponding values for the pipe flow and TBL. This log-law fit is seen to describe the variation for the smooth and rough pipe flows as well as the TBL reasonably well. These values for A_1^m and B_1^m may therefore be considered as approximations to the "universal" log law constants (to within $\pm 6\%$ for A_1^m and $\pm 1\%$ for B_1^m), with intermediate scales, should a universal log law exist for wall turbulence. The values of A_1^m and B_1^m calculated above for different cases have been summarized in table 1.

The classical log-law coefficients, A_1 and B_1 (equation 1) can be readily expressed in terms of A_1^m and B_1^m: it may be rearranged as follows:

$$\left(\frac{\overline{u^2}}{u_m^2}\right)\left(\frac{u_m^2}{u_\tau^2}\right) = B_1 - A_1 \ln\left[\left(\frac{y}{y_m}\right)\left(\frac{y_m}{\delta}\right)\right]. \qquad (3)$$

Here, we take $\delta = R$ for the pipe flow and $\delta = \delta_{99}$ for the TBL. Equation (3) leads to the following relation between the two sets of coefficients:

$$A_1 = A_1^m\left(\frac{u_m^2}{u_\tau^2}\right), \quad B_1 = \left[A_1^m \ln\left(\frac{y_m}{\delta}\right) + B_1^m\right]\left(\frac{u_m^2}{u_\tau^2}\right). \quad (4)$$

Since A_1^m and B_1^m are constants independent of Reynolds number, equation (4) shows the dependence of A_1 and B_1 on the ratios of scaling variables u_m/u_τ and y_m/δ, which are functions of Re_τ. The variation of u_m/u_τ with Re_τ for the smooth pipe and TBL is shown in figure 5(a). For the pipe flow u_m/u_τ continues to increase until $Re_\tau = O(10^5)$, whereas for the TBL it seems to settle down to a more or less constant value for $Re_\tau > 20,000$; for both flows, this ratio exhibits a strong Re-number dependence for $Re_\tau < 20,000$. The Re-number dependence of y_m/δ is clear from its definition: $y_m/\delta = 3.5/\sqrt{Re_\tau}$. This suggests that the classical log-law coefficients A_1 and B_1 should show a systematic Reynolds-number dependence. This expectation is borne out by the variation in value of A_1 and B_1 calculated from equation (4), and plotted in figures 5(b) and (c); for this, we have used $A_1^m = 0.178$ and $B_1^m = 1.005$ for the pipe and $A_1^m = 0.200$ and $B_1^m = 1.028$ for the TBL (table 1). Figure 5(b) shows that there is a significant variation of A_1, i.e. the Townsend-Perry 'constant', for $Re_\tau < 20,000$. For $Re_\tau > 20,000$, A_1 continues to increase for the pipe flow whereas for the TBL, it reaches a relative constant value for $Re_\tau \gtrsim 10,000$. It is interesting to note that, for $Re_\tau > 70,000$, the values of A_1 for the pipe flow and TBL are quite close to each other (in the range $1.23 - 1.24$). Needless to say, the trend in A_1 replicates the trend in u_m/u_τ, by virtue of equation (4). On the other hand, B_1 shows a comparatively larger variation at large Re_τ as seen in figure 5(c).

The log-law fits (equation 1) obtained by using the coefficients shown in figure 5 are plotted in inner variables in figures 6(a) and (b), for pipe flow and TBL respectively. As can be seen, the log-law fits match the data well over the entire Re_τ range for both the flows. Note that these are not individual log-law fits, but those obtained by using A_1 and B_1 calculated from equation (4) for constant values of A_1^m and B_1^m, for each flow. The advantage of this exercise is that, once the limits on y/y_m for the determination of A_1^m and B_1^m are fixed, the extent of the classical log law for the variance is determined automatically (figure 6). In particular, the lower limit of the log law is found to scale on $\sqrt{Re_\tau}$. Figures 5 and 6 confirm the systematic dependence of the Townsend-Perry 'constant' on Reynolds number for the pipe flow and the TBL. However, it is not yet clear whether it has reached an asymptotic value at the highest Reynolds numbers.

DISCUSSION

The present analysis enables us to reconcile the different values for the Townsend-Perry 'constant' reported in the literature. For the pipe flow, we obtain $A_1 = 1.243$ for $Re_\tau = 98,190$ (figure 5b) which is entirely consistent with $A_1 = 1.25$ reported by Hultmark *et al.* (2012) and $A_1 = 1.23 \pm 0.05$ reported by Marusic *et al.* (2013) at the same Reynolds number. Moreover, $A_1 = 0.882$ obtained for $Re_\tau = 3,334$ here for the pipe flow, compares well with $A_1 = 0.9$ for $Re_\tau \leq 3,900$ reported in Perry *et al.* (1986).

With regard to the TBL, Vallikivi *et al.* (2015) found $A_1 = 1.24$ works well for describing the logarithmic profile for the variance for $Re_\tau > 20,000$. The present analysis finds A_1 in the range $1.22 - 1.238$ for $Re_\tau = 25,062 - 72,526$ for the data of VHS (figure 5b) which is consistent with the value of Vallikivi *et al.* (2015). For the highest Reynolds number, the data of MHM ($Re_\tau = 15,685$ based on δ_{99}) give $A_1 = 1.204$, which compares well with

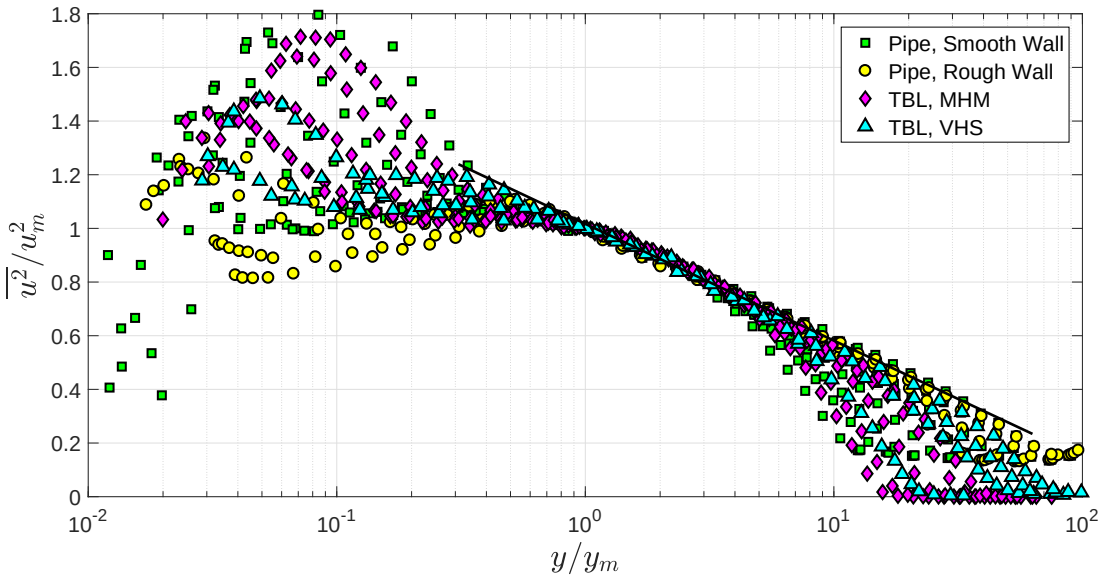

Figure 4. Comparison of the intermediate-scaled streamwise variance profiles for the pipe flow and TBL. The solid line is the log-law fit (equation 2), with averaged values of the constants: $A_1^m = 0.189$ and $B_1^m = 1.017$; see table 1.

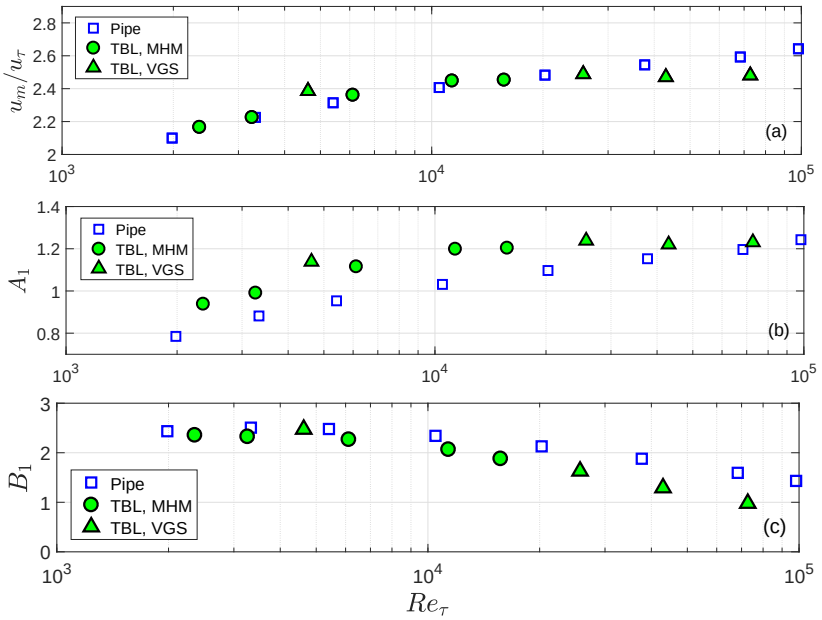

Figure 5. The variation with Re_τ of (a) u_m/u_τ, (b) A_1, (c) B_1; A_1 and B_1 have been calculated from equation (4).

$A_1 = 1.19$ reported by Meneveau & Marusic (2013) at the same Re_τ. At lower Reynolds numbers, Meneveau & Marusic (2013) give $A_1 = 1.25$ for the MHM data, which is much higher than the values obtained here: $0.94 - 1.12$ for $Re_\tau = 2,353 - 6,115$. The higher value of A_1 reported by Meneveau & Marusic (2013) for the lower Re_τ could be attributed to the fact that they used a fixed lower limit of $y^+ = 400$ to fit the log law, whereas the present work uses the lower limit to be proportional to $\sqrt{Re_\tau}$; see also Marusic *et al.* (2013). Note that $A_1 = 0.94 - 1.12$ obtained for $Re_\tau = 2,353 - 6,115$ in this work is entirely consistent with $A_1 = 1.03$ reported by Perry & Li (1990) for $Re_\tau = 1,193 - 4,433$. Finally, Marusic *et al.* (2013) have reported $A_1 = 1.26 \pm 0.06$ for the TBL at $\delta_{99}^+ \approx 15,000$; the present value of 1.204 for a similar Re_τ falls within this uncertainty band (towards the lower end).

The present results clearly have implications for the attached-eddy hypothesis. Marusic *et al.* (2013) argued that the Re_τ-dependence of the lower limit for the log law should not be regarded as incompatible with Townsend's theory; it means that the range of the self-similar attached eddies is given by $l_o \ll y \ll \delta$, with $l_o^+ \sim \sqrt{Re_\tau}$ (Marusic *et al.*, 2013). The same considerations would hold for the present analysis in which the start of the log law scales on $\sqrt{Re_\tau}$. Our main finding, however, is that the range of energy containing eddies, which contribute to the log law (e.g. the type-A eddies in the attached-eddy model; see Marusic & Monty, 2019), appear to scale on the intermediate variables, y_m and u_m, instead of the classical variables δ and u_τ. The success of the intermediate scaling, which provides a local description of the inertial sublayer, supports the self-similar nature of the attached eddies. It is not clear, however, whether the eddies that scale on u_m are physically attached to the wall; see the discussion in Marusic & Monty (2019).

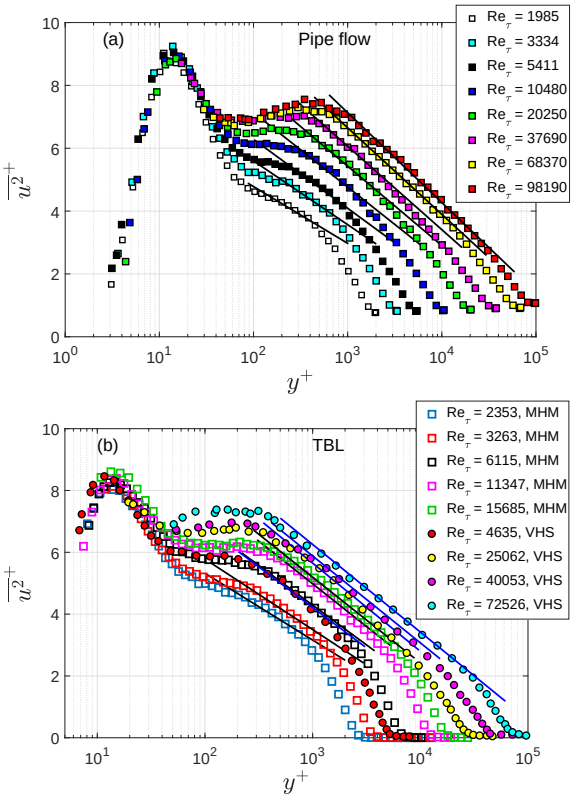

Figure 6. Streamwise variance profiles in inner variables for (a) smooth pipe, (b) TBL. The solid lines are the classical log-law fits (equation 1), using the values of A_1 and B_1 obtained from equation (4) using fixed A_1^m and B_1^m.

It is interesting to note that y_m is typically above the wall-normal location of the outer-spectral peak, where the energy of the very-large-scale motions (VLSMs)/superstructures peak (Vallikivi *et al.*, 2015a). Thus the heirarchy of the VLSMs/superstructures, with progressively decreasing energy with wall-normal distance, could be the plausible candidates for the 'attached' eddies; see also Hwang (2015) for a somewhat different picture of the candidate eddies.

CONCLUSIONS

We have shown that an intermediate length scale, $y_m^+ = 3.5\sqrt{Re_\tau}$, and an associated velocity scale, equal to the rms fluctuating velocity at $y = y_m$, result in a Reynolds-number similarity for the streamwise variance in the intermediate region of the pipe flow as well as the TBL. There exists a Reynolds-number independent logarithmic law in the intermediate-scaled variance, for $y > y_m$, with a *constant* (i.e. Re-number invariant) log-law slope. This translates into a systematic variation of the classical Townsend-Perry 'constant' with Reynolds number for both pipe and TBL. The present analysis provides a framework for reconciling the different values of the Townsend-Perry 'constant' available in the literature - they are most likely due to the different Reynolds numbers used in different studies. The present findings can have interesting implications towards the attached-eddy modelling in wall turbulence, in terms of choosing the scaling and form for the "attached eddies".

ACKNOWLEDGEMENT

We are grateful to Professors Lex Smits and Nicholas Hutchins for sharing their data. We acknowledge financial support from EPSRC under grant no. EP/I037938/1.

REFERENCES

Hultmark, M., Vallikivi, M., Bailey, S. C. C. & Smits, A. J. 2012 Turbulent pipe flow at extreme reynolds numbers. *Phys. Rev. Lett.* **108**, 094501.

Hultmark, M., Vallikivi, M., Bailey, S. C. C. & Smits, A. J. 2013 Logarithmic scaling of turbulence in smooth- and rough-wall pipe flow. *J. Fluid Mech.* **728**, 376–395.

Hwang, Y. 2015 Statistical structure of self-sustaining attached eddies in turbulent channel flow. *J. Fluid Mech.* **767**, 254–289.

Klewicki, J. C. 2013 Self-similar mean dynamics in turbulent wall flows. *J. Fluid Mech.* **718**, 596–621.

Marusic, I. & Monty, J. P. 2019 Attached eddy model of wall turbulence. *Ann. Rev. Fluid Mech.* **51**, 49–74.

Marusic, I., Monty, J. P., Hultmark, M. & Smits, A. J. 2013 On the logarithmic region in wall turbulence. *J. Fluid Mech.* **716**, R3.

Mathis, R., Hutchins, N. & Marusic, I. 2009 Large-scale amplitude modulation of the small-scale structures in turbulent boundary layers. *J. Fluid Mech.* **628**, 311–337.

Meneveau, C. & Marusic, I. 2013 Generalized logarithmic law for high-order moments in turbulent boundary layers. *J. Fluid Mech.* **719**, R1.

Nickels, T. B., Marusic, I., Hafez, S., Hutchins, N. & Chong, M. S. 2007 Some predictions of the attached eddy model for a high reynolds number boundary layer. *Phil. Trans. R. Soc. A* **365**, 807–822.

Perry, A. E. & Chong, M. S. 1982 On the mechanism of wall turbulence. *J. Fluid Mech.* **119**, 173–217.

Perry, A. E., Henbest, S. & Chong, M. S. 1986 A theoretical and experimental study of wall turbulence. *J. Fluid Mech.* **165**, 163–199.

Perry, A. E. & Li, J. D. 1990 Experimental support for the attached-eddy hypothesis in zero-pressure-gradient turbulent boundary layers. *J. Fluid Mech.* **218**, 405–438.

Perry, A. E. & Marusic, I. 1995 A wall-wake model for the turbulence structure of boundary layers. part 1. extension of the attached eddy hypothesis. *J. Fluid Mech.* **298**, 361–388.

Smits, A. J., McKeon, B. J. & Marusic, I. 2011 High-reynolds number wall turbulence. *Ann. Rev. Fluid Mech.* **43**, 353–375.

Sreenivasan, K. R. & Sahay, A. 1997 The persistence of viscous effects in the overlap region, and the mean velocity in turbulent pipe and channel flows. In *Self-Sustaining Mechanisms of Wall Turbulence* (ed. R. Panton), pp. 253–272. Comp. Mech. Publ.

Townsend, A. A. 1976 *The Structure of Turbulent Shear Flow*. Cambridge University Press.

Vallikivi, M., Ganapathisubramani, B. & Smits, A. J. 2015a Spectral scaling in boundary layers and pipes at very high reynolds numbers. *J. Fluid Mech.* **771**, 303–326.

Vallikivi, M., Hultmark, M. & Smits, A. J. 2015 Turbulent boundary layer statistics at very high reynolds number. *J. Fluid Mech.* **779**, 371–389.